First Results from KamLAND

Tadao Mitsui[1] for the KamLAND collaboration
(1) Research Center for Neutrino Science, Faculty of Science, Tohoku University, Sendai 980-8578, Japan

Abstract

KamLAND has measured the flux of $\bar{\nu}_e$'s from distant nuclear reactors. We find the ratio of the observed $\bar{\nu}_e$ events to the number expected in the absence of disappearance is $0.611 \pm 0.085(\text{stat}) \pm 0.041(\text{syst})$ for $\bar{\nu}_e$ energies > 3.4 MeV, thus excluding the standard $\bar{\nu}_e$ propagation at 99.95% C.L. Assuming two-flavor neutrino oscillations and CPT invariance, all solutions to the solar neutrino problem except for the "large mixing angle" region are excluded. Future KamLAND measurements will provide precision determinations of neutrino oscillation parameters and first opportunity to observe "geoneutrinos" from the Earth's interior.

1. Introduction

Nuclear reactors are the oldest and the most precisely understood neutrino ($\bar{\nu}_e$) sources. Although discoveries and implications on neutrino masses and mixings have been provided by "celestial" sources, i.e., solar and atmospheric (cosmic-ray origin) neutrinos, the oldest artificial sources should still play an important role in obtaining firm information.

The primary goal of the Kamioka Liquid Scintillator Anti-Neutrino Detector (KamLAND) is a search for reactor-$\bar{\nu}_e$ oscillation. The long baseline, typically 180 km, enables us to address the oscillation solution of the solar neutrino problem. The inverse β-decay reaction, $\bar{\nu}_e + p \rightarrow e^+ + n$ is used to detect $\bar{\nu}_e$'s in liquid scintillator (LS). Detecting both the e^+ and the delayed 2.2 MeV γ-ray from neutron capture on a proton is a powerful tool for reducing background.

The detector and analyses shown here are our first results published in [1]. The neutrino detector/target of 1-kton ultrapure LS is contained in a 13-m-diameter plastic balloon. A buffer of minerarl oil between the balloon and an 18-m-diameter spherical stainless-steel containment vessel shields the LS from external radiation. A 1879 photomultiplier tube (PMT) array, mounted on the vessel, completes the inner detector (ID), which is surrounded by a 3.2 kton water-Cherenkov detector to tag cosmic-ray muons. The primary ID trigger threshold is ~ 0.7 MeV. Energy response in the 0.5 to 7.5 MeV range is calibrated with ^{68}Ge, ^{65}Zn, ^{60}Co, and Am-Be γ sources. The observed energy resolution is

pp. 1221–1224

$\sim 7.5\%/\sqrt{E(\mathrm{MeV})}$. Event locations are reconstructed from the timing of PMT hits with a systematic error ~ 5 cm and the typical resolution ~ 25 cm.

2. Evidence for Reactor Antineutrino Disappearance

The data shown here were collected from March 4 through October 6, 2002. We obtained 370×10^6 events in 145.1 d of live time. After selection cuts, such as fiducial volume ($R < 5$ m), time/vertex correlation between prompt (e^+) and delayed (2.2-MeV γ) events etc, total exposure and cut efficiency are 162 ton·yr and (78.3±1.6)% respectively. Fig. 1 (left bottom panel) shows prompt energy spectrum after those cuts. Below 2.6 MeV ($\bar{\nu}_e$ energy 3.4 MeV), "geo-$\bar{\nu}_e$'s" are expected as described in the next section, then counting above it, 54 events are identified as reactor-$\bar{\nu}_e$. The corresponding expected number of events without disappearance is 86.8 ± 5.6 calculated from thermal power, burnup, and fuel exchange records provided by Electric Power Companies. Expected number of background events is 1±1, mainly from ^{8}He and ^{9}Li which emit both e^- and n. The ratio of observed to expected events is then, $0.611 \pm 0.085(\mathrm{stat}) \pm 0.041(\mathrm{syst})$, excluding $\bar{\nu}_e$ propagation without disappearance at 99.95% C.L.

The neutrino oscillation parameter region for two-neutrino mixing is shown in Fig. 1 (right panel); the excluded region by event rate and the allowed region by spectral shape analysis. The latter is powerful since the flux is dominated by a few reactors around 180 km. Assuming CPT invariance, LMA is the only oscillation solution of the solar neutrino problem consistent with the present result.

An analysis with a 0.9 MeV threshold (not shown) is consistent with the above result, in which the number of geo-$\bar{\nu}_e$ events for the best fit are 4 for ^{238}U and 5 for ^{232}Th, with no statistical significance though. The corresponding allowed range of the heat source is 0 to 110 TW at 95% C.L. under the model Ia in [3]. In our future measurements, significant geo-$\bar{\nu}_e$ flux or a strong upper limit will be obtained as well as precise determination of neutrino oscillation parameters.

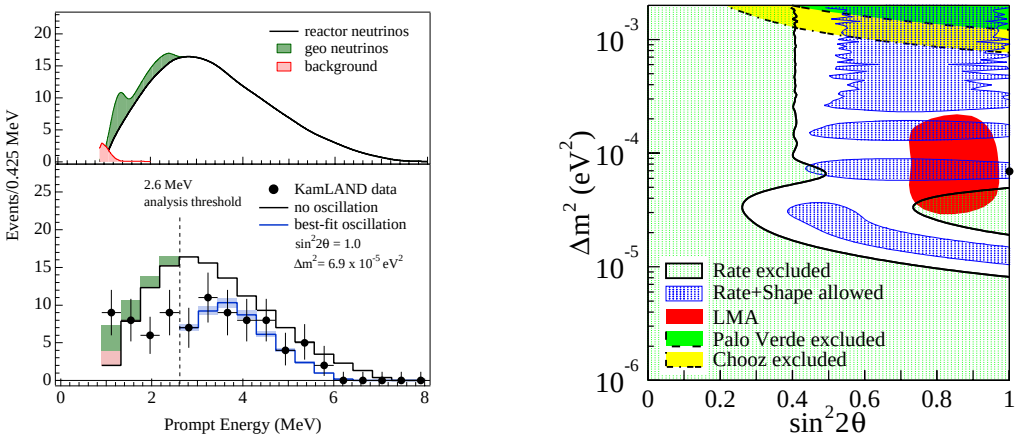

Fig. 1. Left panels: Expected and observed prompt energy spectra. Right panel: Excluded and allowed regions of neutrino oscillation parameters at 95% C.L.

3. Toward Geoneutrino Observation

Neutrinos (geo-$\bar{\nu}_e$'s) from decay of ^{238}U and ^{232}Th in the Earth [3] are expected as a new probe of geophysics. It is considered radiogenic heat from those elements considerably ($\sim 40\%$) contributes to the total heat source (~ 40 TW) of the Earth. Although its amount is quit important in studying origin of the Earth, no direct probe to the inside source has been available so far.

The relation between geo-$\bar{\nu}_e$ flux F and total radiogenic heat Q is written as $F = G/(4\pi R^2) \cdot (n_\nu/q)Q$, where R is the radius of the Earth, n_ν and q are respectively the number of neutrinos and heat production per decay. The dimensionless factor G is determined only by distribution of the elements not depending on their total amounts, e.g., $G = 1.5$ for uniform distribution throughout the Earth. Using cross sections of $\bar{\nu}_e$ detection and number of target protons [1], the expected event rates at KamLAND are then, $N_{\rm U} = 1.58\,[{\rm kt}^{-1}\,{\rm y}^{-1}\,{\rm TW}^{-1}] \times Q_{\rm U}[{\rm TW}] \times G_{\rm U}$ and $N_{\rm Th} = 0.45\,[{\rm kt}^{-1}\,{\rm y}^{-1}\,{\rm TW}^{-1}] \times Q_{\rm Th}[{\rm TW}] \times G_{\rm Th}$ for geo-$\bar{\nu}_e$'s from U and Th respectively. For example, assuming $G_{\rm U} = G_{\rm Th} = 2.8$ (Fig. 3, shown later) and $Q_{\rm U} = Q_{\rm Th} = 8$ TW, then 45 events/kt·y is expected being consistent with previous predictions [3]. Those simple relations tell us that if we can estimate G with reasonable precision, our observation is translated as heat source measurement. Note that geo-$\bar{\nu}_e$ oscillation can essentially be approximated by constant suppression with a factor $1 - 1/2\sin^2 2\theta$ which is determined by reactor-$\bar{\nu}_e$ analysis.

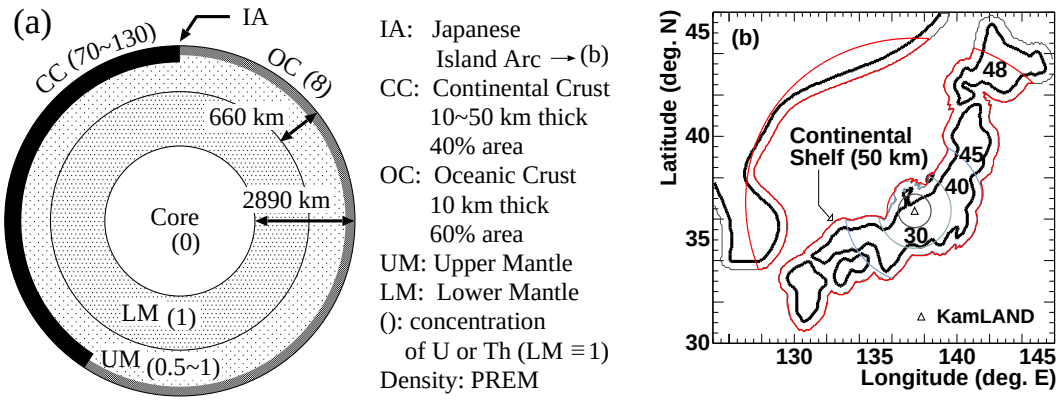

Fig. 2. Modeled distribution of U and Th. (a) Global distribution. (b) Near field. Crusts under the land and continental shelf are the same as CC, while other region OC. Contours show percentages of crust contribution to the total geo-$\bar{\nu}_e$ flux when thickness is 30 km, concentration 100, and continental shelf of a width 50 km.

The distribution of U and Th are considered similar and here modeled as shown in Fig. 2, based on geophysical studies [2, 3]. Since G doesn't depend on the total amounts, concentrations of the elements (U or Th) are normalized to 1 at lower mantle (LM). We will test more than one values for some parameters

being ambiguous and effective to G, i.e., thicknesses of continental crust (CC) and the crust under Japanese Island Arc (IA), as well as concentrations there. G is numerically calculated as $G = \int r^{-2}\rho dV/(\int R^{-2}\rho dV)$, where $\rho = \rho(x)$ is the density multiplied by concentration, and r the distance between x and the observation point. Fig. 3 shows resultant G values as a function of model parameters. G variation is the largest when only near field is modified (Fig. 3(c)), while other ambiguities are relatively small (Fig. 3(b)), which is natural considering that about one half of geo-$\bar{\nu}_e$'s come from IA crust (Fig. 2(b), Fig. 3(a)). Closer geo-physical and -chemical studies on near field, however, will reduce those ambiguities, by which together with more statistics, we aim at first geo-$\bar{\nu}_e$ observation, flux measurement, and addressing the radiogenic heat source of the Earth.

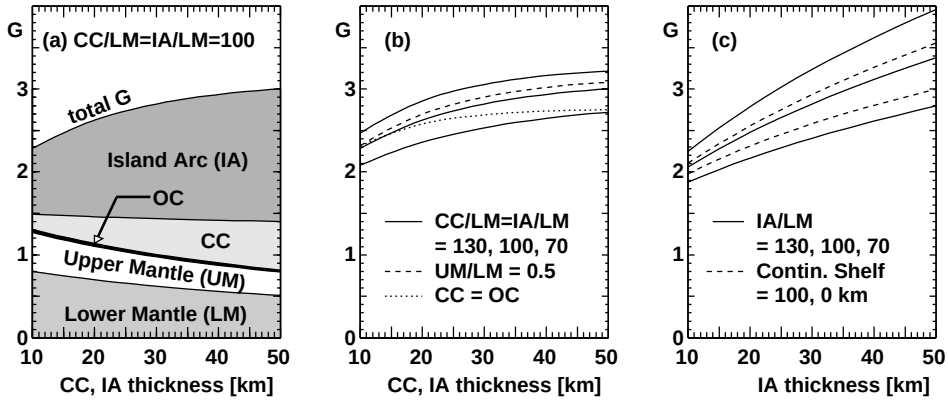

Fig. 3. G dependence on parameters. (a) Dependence on crust thickness. OC is fixed because its contribution is very small as seen. (b) Also concentrations changed (solid lines). Dashed line: reduced concentration in upper mantle (UM), corresponding to the case U and Th are depleted only from UM (all the other results: UM/LM= 1). Dotted line: uniform crust. (c) Cases IA is different from other CC. (other CC fixed: 30 km thick, concentration 100). Dashed lines: width of the continental shelf: 0, 100 km. (all the other results: 50 km).

Sincere gratitude is to the staffs of ICRC2003, also to all the KamLAND collaborators and Professor E. Ohtani for valuable discussions. KamLAND project is supported by the Japanese Ministry of Education, Culture, Sports, Science and Technology and the United States Department of Energy. The reactor data are provided courtesy of the Electric Power Companies and associations in Japan.

1. Eguchi K. et al. (KamLAND collaboration) 2003, PRL 90, 021802
2. Ohtani E. 2002, Proc. 1st Sendai Intern. Conf. on Neutrino Science
3. Raghavan R.S., Schoenert S., Enomoto S., Shirai J., Suekane F. Suzuki A. 1998, PRL 80, 635, and references therein